Influence of spraying distance and post-cooling on cryogen spray cooling for dermatologic laser surgery

Guillermo Aguilar[1,2], Boris Majaron[2,3], John A. Viator[2], Brooke Basinger[2], Emil Karapetian[4], Lars. O. Svaasand[2,5], Enrique J. Lavernia[4] and J. Stuart Nelson[1,2]

[1] Whitaker Center for Biomedical Engineering, University of California, Irvine, CA 92612
[2] Beckman Laser Institute and Medical Clinic, University of California, Irvine, CA 92612
[3] Jožef Stefan Institute, Jamova 39, SI-1000 Ljubljana, Slovenia
[4] Department of Chemical and Biochemical Engineering and Materials Science, University of California, Irvine, CA 92697
[5] Dept. of Physical Electronics, Norwegian Univ. of Science and Technology, 7491 Trondheim, Norway

ABSTRACT

Cryogen spray cooling (CSC) is used to minimize the risk of epidermal damage in various laser dermatological procedures such as treatment of port wine stain birthmarks and hair removal. However, the spray characteristics and combination of CSC and heating (laser) to obtain optimal treatments have not yet been determined.
The distance between the nozzle tip and the skin surface for commercial devices was apparently chosen based on the position at which the cryogen spray reached a minimum temperature, presumably with the expectation that such a minimum would correspond to maximal heat flux. We have systematically measured spray characteristics of various nozzles, such as mean droplet diameter, velocity, temperature, and heat transfer coefficient, as a function of distance from the nozzle tip. Among other interesting correlations between these spray characteristics, it is shown that, for nozzle-to-skin distances between 20 to 80 mm, variations in the heat transfer coefficient are larger than those in the spray temperature and, therefore, maximization of the heat flux should be better dictated by the distance at which the heat transfer coefficient is maximized rather than that at which the spray temperature is minimized. Also, the influence of droplet diameter appears to be more influential on the heat transfer coefficient value than that of droplet velocity. Based on spray characteristic correlations, different ranges for positioning the nozzles are recommended, depending on the clinical application. Also, a 2D finite-difference method has been developed to study the spatial and temporal thermal variations within the skin. Our results show that it is possible to decrease significantly the epidermal damage after laser irradiation provided the heat transfer coefficient is significantly increased. The influence of post-cooling has minimal effects for the cases studied.

1. INTRODUCTION

Cryogen spray cooling (CSC) has been used effectively to cool selectively the epidermis while minimally cooling deeper targets[1] during laser therapy of several dermatoses, such as port wine stains (PWS) birthmarks[2,3], and cosmetic treatments, such as hair removal[4]. However, to obtain optimal cooling selectivity, the amount of heat removed through the skin surface should be properly controlled. For shallow targets, such as PWS, commercial cryogen spurts do not seem to provide sufficient epidermal protection for skin types with relatively high melanin content (e.g., types III and higher), where an increase of dosage is needed to cause complete photocoagulation of blood vessels. On the other hand, a recent study has indicated that the heat extraction rates produced by commercial devices aimed at deeper targets, e.g., hair follicles, may be unnecessarily large[5].

Some advances have been made in terms of optimizing spurt durations to provide better cooling selectivity. A recent study has revealed that cryogen spurts of 100-200 ms could result in better epidermal protection than that provided by 30 to 50 ms spurts[1]. Spurts of similar duration have served to increase the threshold of epidermal damage on non-PWS human cadaver skin by a factor of three[6]. Nevertheless, more work is required to better understand how different nozzles and spraying conditions affect spray characteristics, such as droplet diameter (D), velocity (V), and temperature (T)[7,8,9], and how these, in turn, affect the heat extraction rate which is ultimately dictated by the skin surface temperature (T_s) and the interface heat transfer coefficient (h).

Optimization of CSC parameters is the first step towards an improvement of dermatologic laser treatments. However, a complete assessment of the extent of epidermal and target damage also requires the analysis of laser irradiation parameters, as well as skin optical and thermal properties. As a first approximation, such an assessment can be made through the use of numerical models to determine the spatial and time dependent temperature fields within the skin during CSC and laser irradiation. Paithankar et al.[10] and Pfefer et al.[11], among others, have recently shown that such models have significant potential as a tool for optimizing heating and cooling parameters.

In this work we determine the effects of nozzle diameter and nozzle-to-skin distance, z, of four spray nozzles varying from 0.5 to 1.4 mm in inner diameter (I.D.) based on the dependence on z of the average values of D, V, T, and h, at the cryogen-substrate interface. Secondly, a 2-D Monte Carlo multi-layer model[12] and a custom-made 2D finite-difference heat diffusion model are used to calculate the light distribution within tissue and the heat diffusion as a function of time, respectively. With the use of both models, and an Arrhenius-type kinetic model used to assess the epidermal and blood vessel damages, we study the influence of the heat transfer coefficient and post-cooling in PWS laser therapy.

2. MATERIALS AND METHODS

Spray Formation

A total of four nozzles were used for this study: Two commercial cryogen spray nozzles used for laser treatment of vascular lesions and hair removal (ScleroPLUS^{TM} (SP), and GentleLASE^{TM} (GL), Candela, Wayland, MA), with approximate inner diameters of 0.8 and 0.5 mm, respectively; and two custom made nozzles (narrow nozzle, N, and wide nozzle, W) of 0.7 and 1.4 mm I.D. Liquid cryogen (tetrafluoroethane, R-134a, boiling temperature, $T_b = -26^oC$, at atmospheric pressure) was delivered through a standard high-pressure hose connecting the container to a control valve. The container is pressurized at the saturation pressure of this cryogen (6.7 bar at 25^{o}C). Spurt durations—defined by the time the valve remains open, were electronically controlled. In this study, we have characterized sprays that were at least 50 ms long, so only characteristics of fully developed sprays were considered[13,16], *i.e.*, sprays that do not vary with time.

Droplet Size and Velocity Measurements

An Ensemble Particle Concentration & Sizing apparatus (EPCS by Insitec/Malvern, Worcestershire,UK) was used to measure average diameters (D) of the spray droplets. This instrument is based on the principle of diffraction of a parallel beam of monochromatic light (provided by a 670 nm diode laser) caused by the obstruction of spray droplets with the beam. When this happens, a diffraction pattern made of a series of alternate light and dark concentric rings (Fraunhofer diffraction) is formed, and the spacing between these rings is related to droplet diameter. A more detailed description may be found in Lefevbre[14]. In order to obtain more localized measurements of D, the beam was reduced from its normal diameter of 10 mm to 3.3 mm with the aid of an inverted beam expander (OptoSigma, Santa Ana, CA). A positioning system was used to displace the nozzle tip perpendicularly to the laser beam, from 15 to 200 mm. In addition, a Phase Doppler Particle Analyzer (PDPA by TSI, St. Paul, MN) was utilized to provide statistical averages of both droplet diameters (D) and velocities (V). PDPA captures and analyzes light scattered by droplets traveling through interfering laser beams of different wavelengths, focused on a probe volume, typically smaller than 1 mm^3. When droplets interfere with these beams, they generate a Doppler signal with a frequency shift proportional to droplet velocity. The phase difference between the signals collected by two adjacent detectors is proportional to droplet diameter.

Temperature Measurements

A type-K thermocouple with bead diameter of approximately 0.3 mm (5SC-TT-E-36 by Omega, Stamford, CT) was used to measure average spray temperature as a function of distance from the nozzle tip, $T(z)$. Cryogen spurt durations of at least 1 second were used, which ensured steady state conditions for the thermocouple. The temperature sensor was supported by a rigid stick and inserted into the center of the spray cone at varying distances from the nozzle. The estimated uncertainty in nozzle-to-skin distance, z, is $\pm$ 0.5 mm. Since water condensation and freezing on the thermocouple bead could affect temperature measurements, these experiments were conducted in a chamber filled with dry air (relative humidity below 5%). Under such conditions, most of the tests did not show appreciable condensation, except for $z > 100$ mm, where signs of frost formation were observed on the thermocouple bead.

Heat transfer coefficient measurements

A custom-made device was built to measure the heat transfer coefficient (h). In short, the device consists of a silver disk (10.48 mm diameter, 0.42 mm thickness), embedded in a thermal insulator, *e.g.*, epoxy. The upper surface of the disk is exposed to the cryogen spray, and the disk temperature is monitored by a type-K thermocouple attached to its lower surface. The energy equation, which describes the disk temperature evolution is:

$$\rho_m C_m V_m \frac{dT}{dt} = A_m\, h (T - T_{cryo}) \quad (1)$$

where ρ_m, C_m, V_m and A_m are the density, specific heat, volume, and exposed surface area of the metallic disk, respectively; h is the heat transfer coefficient, and T and T_{cryo} are the temperatures of the disk and the cryogen, respectively. This equation assumes that T is uniform over the whole disk at any given time. This assumption means that the disk relaxation time—given by $(\rho_m\ V_m\ C_m)/(A_m\ h)$, is much larger than the diffusion time across the disk thickness, d_m^2/α, where d_m is the disk thickness and α its thermal diffusivity. Substituting T_{cryo} with measured spray temperature, h can be calculated from measurements of disk temperature during CSC.

Numerical Simulation of Energy Absorption and Cryogen Spray Cooling

A numerical model was developed using a 2D finite-difference (FD) approximation to the heat equation in cylindrical coordinates. The cross section area of the skin model was 15 mm wide and 1mm thick, and was discretized into 61 nodes spaced 250 μm in the radial direction and 101 nodes spaced 10 μm in the axial direction. Time steps of 100 μs ensured stability and convergence criteria. Starting with a constant temperature of 35°C, the temperature field resulting from a 100 ms spurt was first computed by imposing a constant convective boundary condition at the skin surface (constant h and constant T_{cryo}). Values of h used in this study varied from 2,400 to 30,000 W/m^2 K, and T_{cryo} was fixed at -58°C. No delay between the end of the spurt and the beginning of the laser pulse was allowed, as suggested by Verkruysse et al.[1]. Then, a source term (q) was incorporated into the heat diffusion model (Eq. 2) to simulate the energy absorption of the laser pulse by epidermal melanin and PWS.

$$\frac{1}{\alpha}\frac{\partial T}{\partial t} = \nabla^2 T + \frac{q}{k} \quad (2)$$

The source term, q, was previously generated using MCML, a Monte Carlo software package developed by Wang *et. al.*[12]. Given the specific optical properties of the skin layers and the geometry and energy of the laser beam, MCML determined the optical transport of photons in the skin layers. For consistency, the skin layer depths and optical properties, as well as the thermal properties we used in this study are the same as those used by Pfefer et al.[11], and are listed in Tables 1 and 2, respectively. All Monte Carlo simulations used four layers: an epidermal melanin layer, a normal dermis layer, a PWS layer, and another normal dermis layer with the same optical and thermal properties as the second layer (Fig. 1). The absorption coefficients (μ_a) of the epidermal layers were set to 8, 20, and 52 cm^{-1}, to describe skin types ranging from light skin to olive skin. These absorption coefficients corresponded to melanin volume fractions of 2, 5, and 13%, respectively, assuming a melanin absorption coefficient of 400 cm^{-1} at 585 nm wavelength[15]. For the normal dermis and blood energy absorption coefficients we used 2.4 and 19.1 cm^{-1}, respectively. The latter values were used in all simulations. Scattering coefficients (μ_s), scattering anisotropies (g), and indices of refraction (n) used for all layers are also listed in Table 1. All simulations used 100,000 photons. The grid spacing for the MCML simulation was the same as that of the FD heat diffusion model. The adjunct program to MCML, CONV, was used to take the infinitesimally narrow photon beam from the MCML simulations and create a flat top, circular beam with 5 mm diameter.

Table 1: Thickness and optical properties of the layers modeled with MCML

layer	thickness (μm)	μ_a (cm^{-1})	μ_s (cm^{-1})	g	n
epidermis	50	8, 20, 52	470	0.79	1.37
dermis	150	2.4	129	0.79	1.37
PWS	200	19.1	467	0.99	1.33
dermis	>> 1,000	2.4	129	0.79	1.37

Table 2: Thermal properties of skin layers used in heat diffusion FD calculations

layer	k [W/(m K)]	ρ [kg/m^3]	c [J/(kg K)]
epidermis	0.21	1,200	3,600
dermis	0.53	1,200	3,800
PWS	0.55	1,100	3,600

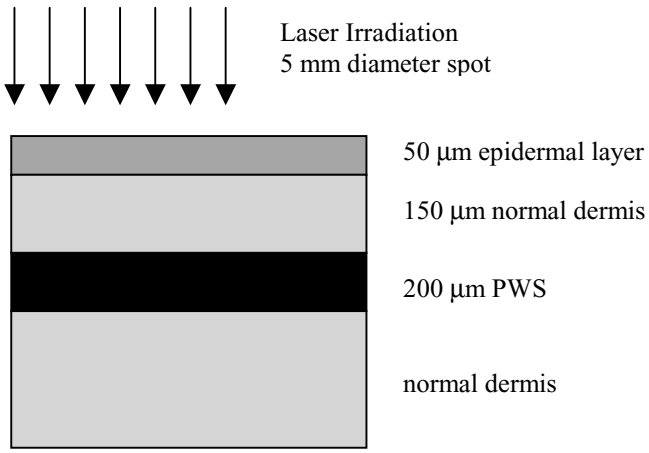

Figure 1: The four layer model used in the numerical simulation.

Assessment of Tissue Thermal Damage

Tissue thermal damage was computed using the Arrhenius-type kinetic model, given by Eq. 3, as follows:

$$\Omega(t) = \int_0^t A \exp(-E_a / RT)\, dt \qquad (3)$$

where A is a frequency factor [1/s], E_a an activation energy barrier [J/mole], R the universal gas constant [8.32 J/mole K], and T the absolute temperature [K]. The parameters A and E_a used in this study are listed in Table 3, and also correspond to the values used in Pfefer et al.[11].

Table 3: Arrhenius damage process coefficients

	A [1/s]	**E_a [J/mole]**
Bulk Skin	7.6×10^{76}	550,000
Hemoglobin	7.6×10^{66}	455,000

3. RESULTS

Nozzle Positioning

Figure 2 shows the average droplet diameter (D), velocity (V), temperature (T) and heat transfer coefficient (h) as a function of z for sprays from all four nozzles. As seen in Figure 2a, the maximum droplet diameter for the nozzles with inner diameters between 0.5 and 0.8 mm, i.e., SP, GL, and N, is D_{max} = 8.7 ± 0.2 μm, measured at z = 60-70 mm. In contrast, D measurements for the 1.4 mm nozzle (W) vary between 12 to 14 μm. The measurements of V for all nozzles are presented in Figure 2b. Although to a different extent, these results show a similar behavior to that of D, with an increasing trend within the first 40 mm from the nozzle. At greater distances, V monotonically decreases, reaching 15 m/s at z = 200 mm in all cases. Measurements of T are depicted in Figure 2c. The temperature trends indicate that the exit temperature, T_0, may gradually vary between –26 °C for the 1.4 mm nozzle (W), to -50 °C for the 0.5 mm nozzle (GL). The minimum temperature, T_{min}, for the nozzles with inner diameters between 0.5 and 0.8 mm is around –58 °C, reached at z = 60-120 mm, and it is slightly lower than T_{min} for the W nozzle at the same z. For the SP, GL and N nozzles, T starts to increase between z = 80 -120 mm, indicating evaporation of cryogen droplets at such distances. Finally, Figure 2d shows the variation of h with z. The measurements for SP and GL were carried out using the method described above, and the values shown represent averages over the duration of the spurt (100 ms) as well as over the detector area. The h value for the W nozzle is a conservative estimate of the range of values reported in Verkruysse et al.[7] (5,900 - 30,000 W/m^{2}K). Measurements of those values, however, were carried out with a different procedure described therein (epoxy block / dynamical method), and the measurements were only taken between z = 50-60 mm. Table 4 summarizes some relevant values of all measured variables.

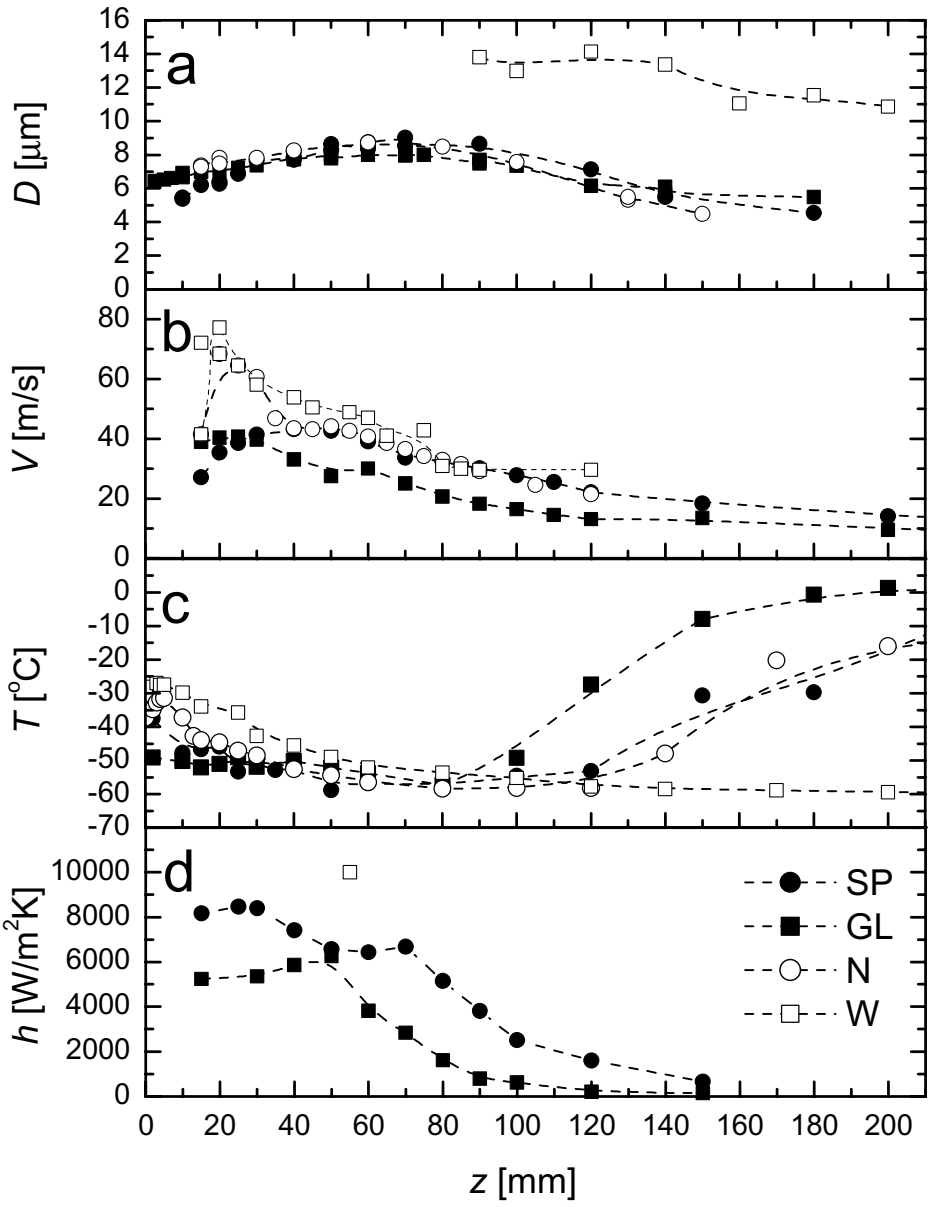

Figure 2: Average droplet diameter (*D*), velocity (*V*), temperature (*T*) and heat transfer coefficient (*h*), measured as a function of distance from the nozzle tip (*z*) for the SP, GL, N, and W nozzles.

Table 4: Relevant values of average droplet diameter (*D*), velocity (*V*), temperature (*T*) and heat transfer coefficient (*h*)

Variable	ScleroPLUS™ (SP) (I.D.= 0.8 mm)	GentleLASE™ (GL) (I.D. = 0.5 mm)	Narrow nozzle (N) (I.D. = 0.7 mm)	Wide Nozzle (W) (I.D. = 1.4 mm)
D_{max} [μm]	8.7	8	8.8	14.1
V_{max} [m/s]	45	42	70	--
T_{min} [°C]	-58	-58	-58	-60
T_0 [°C]	-37	-48	-38	-26
h_{max} [W/m² K]	8,400	6,200	--	10,000

Numerical Simulations

Effect of *h* on light skin (μ_a = 8 cm^{-1}) PWS laser therapy

Figure 3 shows the temperature profiles computed for the lightest skin type chosen for this study (μ_a = 8 cm^{-1}). The dotted lines represent temperature as a function of depth at the end of 100 ms spurts for two cases: h = 2,400 W/m^{2}K, which is the lowest value of h for CSC reported in the literature[3], and h = 6,000 W/m^{2}K, which is a conservative value corresponding to the measurements presented above. In both cases, cryogen temperature, T_{cryo}, was –58 °C, i.e., the minimum spray temperature measured for the SP, GL, and N sprays. The dashed and solid lines represent, respectively, temperature profiles at the end of 1.5 ms laser pulses with a fluence of 12 J/cm^2 for each of the values of h.

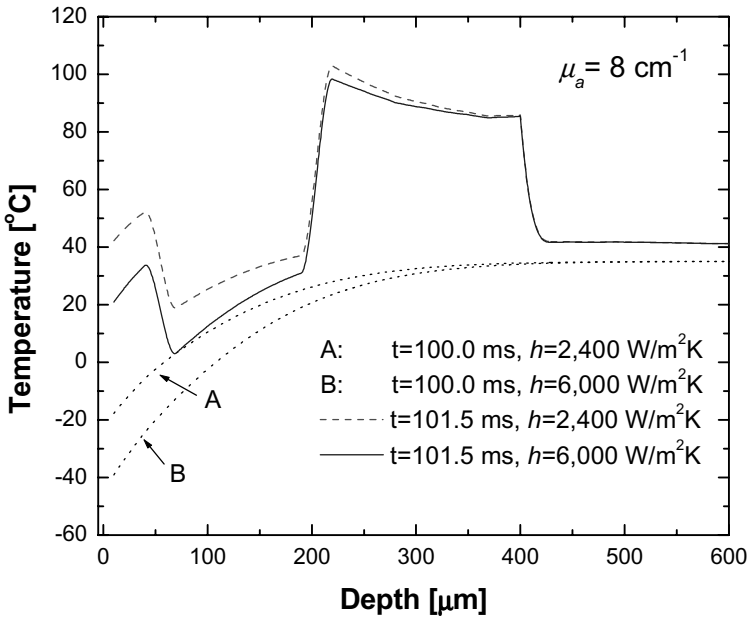

Figure 3: Skin temperature profiles as a function of depth computed using a 2D finite-difference simulation. Spurt duration: 100 ms. No delay between cryogen pre-cooling spurt and a 585 nm wavelength, 1.5 ms laser pulse. Epidermal absorption coefficient: 8 cm^{-1}. Fluence: 12 J/cm^2. T_{cryo} = –58 °C.

Effect of post-cooling on tanned light skin (μ_a = 20 cm^{-1}) PWS laser therapy

Figure 4 shows the results of temperature profiles computed for μ_a = 20 cm^{-1}, i.e., for the mid-tanned light skin chosen for this study. The dotted line represents temperature as a function of depth at the end of a 1.5 ms laser pulse with a fluence of 13 J/cm^2. Prior to this pulse, a 100 ms spurt with a heat transfer coefficient, h, of 8,400 W/m^{2}K was imposed. According to the measurements shown above, this is the maximum value of h that could be obtained with the SP nozzle if it was positioned at 30 mm from the skin surface (Fig. 2d). The dashed and solid lines represent the temperature profiles 12.5 ms after the end of the laser pulse (114.0 ms from start of pre-cooling), when no post-cooling and post-cooling are applied, respectively.

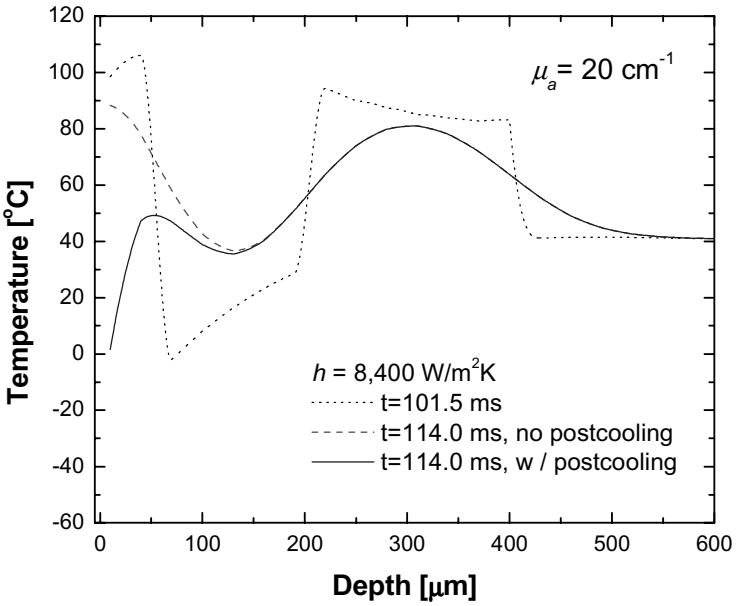

Figure 4: Skin temperature profiles as a function of depth computed using a 2D finite-difference simulation. Spurt duration: 100 ms. No delay between cryogen pre-cooling spurt and a 585 nm wavelength, 1.5 ms laser pulse. Epidermal absorption coefficient: 20 cm^{-1}. Fluence: 13 J/cm^2. T_{cryo} = –58 °C.

Effect of h on tanned light skin (μ_a = 20 cm^{-1}) PWS laser therapy

Figure 5 shows temperature profiles computed for the same skin-type shown in Fig. 4 (μ_a = 20 cm^{-1}), i.e., for the mid-tanned skin-type chosen for this study. The dotted lines represent temperature as a function of depth at the end of 1.5 ms laser pulses with a fluence of 13 J/cm^2. Prior to these pulses, 100 ms spurts with heat transfer coefficients of 8,400 W/m^{2}K and 30,000 W/m^{2}K were imposed, respectively. The latter value of h was chosen as an extreme upper limit, which would be desirable to reach to optimize epidermal protection. In both cases, cryogen temperature, T_{cryo}, was fixed at –58 °C. The dashed and solid lines represent the temperature profiles 4.5 ms after the end of the laser pulses for each of the values of h. Post-cooling was applied in both cases with identical values of h to those used during the pre-cooling.

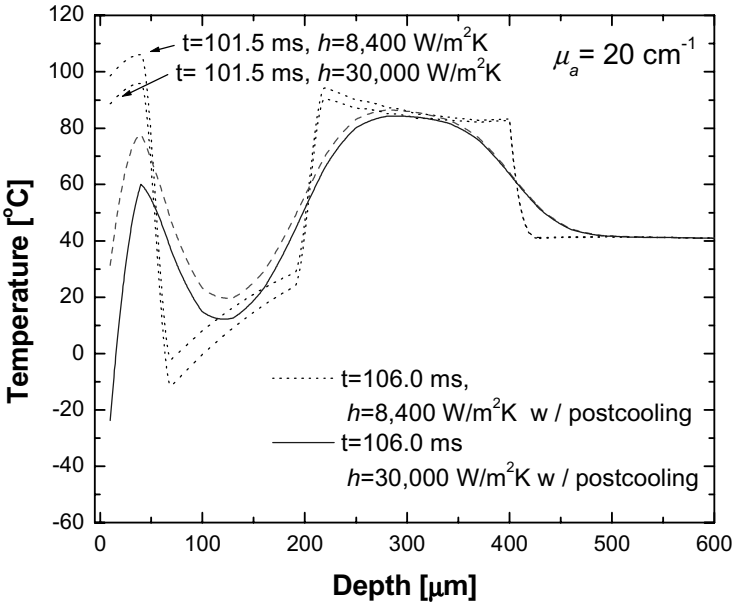

Figure 5: Skin temperature profiles as a function of depth computed using a 2D finite-difference simulation. Spurt duration: 100 ms. No delay between cryogen pre-cooling spurt and a 585 nm wavelength, 1.5 ms laser pulse. Epidermal absorption coefficient: 20 cm^{-1}. Fluence: 13 J/cm^2. T_{cryo} = –58 °C.

Effect of h and post-cooling in olive skin (μ_a = 52 cm^{-1}) PWS laser therapy

Figure 6 shows temperature profiles computed for the darkest skin-type chosen for this study (μ_a = 52 cm^{-1}). The dotted lines represent temperature as a function of depth at the end of 1.5 ms laser pulses with a fluence of 10 J/cm^2. Prior to these pulses,

100 ms spurts with heat transfer coefficients of 8,400 W/m^{2}K and 60,000 W/m^{2}K were imposed, respectively. Clearly, the temperature reached is excessively high within the epidermis, and no correction is made to take into account phase and chemical changes that would likely occur after such a large energy absorption. The dashed and solid lines represent the temperature profiles 12.5 ms after the end of the laser pulses for each of the values of *h*. In both cases, post-cooling (PC) is applied with identical values of *h* to those used during the pre-cooling, i.e., 8,400 and 60,000 W/m^{2}K, respectively.

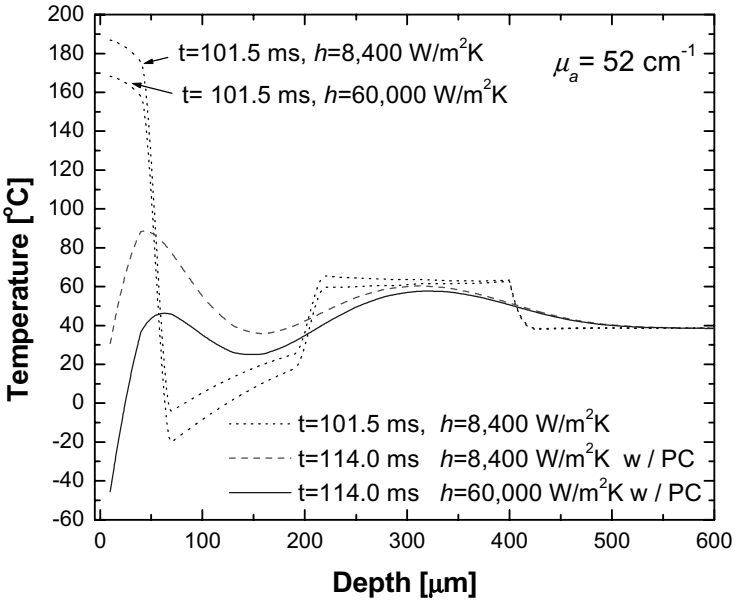

Figure 6: Skin temperature profiles as a function of depth computed using a 2D finite-difference simulation. Spurt duration: 100 ms. No delay between cryogen pre-cooling spurt and a 585 nm, 1.5 ms laser pulse. Epidermal absorption coefficient: 52 cm^{-1}. Fluence: 10 J/cm^2. T_{cryo} = –58 °C

Finally, Table 5 shows values of Ω computed from Eq. 3 to assess the levels of epidermal (Ω_E) and PWS (Ω_{PWS}) damages for the cases shown in Figs. 3-6. Also, the ratios between the epidermal damages were calculated to qualitatively represent the effects of increasing heat transfer coefficients and benefits of use of post-cooling.

Table 5. Values of Ω computed from Eq. 3 for epidermal damages (Ω_E) corresponding to results represented in Figs. 4-5.

	Ω_E	$\Omega_{E,1}/\Omega_{E,2}$	Ω_{PWS}	$\Omega_{PWS,1}/\Omega_{PWS,2}$
Fig. 3 (μ_a=8 cm^{-1})				
1) *h* = 2,400, no PC	negligible		1,200	
				2.0
2) *h* = 6,000 no PC	negligible		600	
Fig. 4 (μ_a=20 cm^{-1})				
1) *h* = 8,400, no PC	7.14		198	
		1.02		1.0
2) *h* = 8,400 PC	7.02		198	
Fig. 5 (μ_a=20 cm^{-1})				
1) *h* = 8,400, PC	7.02		198	
		175		2.4
2) *h* = 30,000, PC	0.04		83	
Fig. 6 (μ_a=52 cm^{-1})				
1) *h* = 8,400, PC	Infinite		0.0085	
				2.7
2) *h* = 60,000, PC	Infinite		0.0032	

4. DISCUSSION

Various features may be pointed out in Fig. 2. First, for the driving pressure corresponding to this cryogen (6.7 bar), nozzles with I.D. between 0.5 to 0.8 mm do not produce significant differences in terms of average droplet diameters, as illustrated in Fig. 2a. This is also evident in spray images reported recently in Aguilar et al.[16]. In contrast, for the 1.4 mm I.D. nozzle (W), droplet diameters are about twice as large throughout the range measured. It was not possible to obtain reliable diameter measurements closer than 90 mm from the nozzle tip for this nozzle. This is because of a high droplet density spray, or even an unbroken jet[16]. The droplet diameter growth seen in Figure 2a between $0 < z < 60$ mm for the SP, GL, and N nozzles, is an indication of droplet coalescence[17,18], a phenomenon which may contribute more to the average droplet diameter variation than the evaporation process[9]. However, evaporation becomes the dominant process in determining average droplet size for $z > 60$ mm, as demonstrated by decreasing D at greater z.

For all nozzles shown in Fig. 2b there is an increase in V within the first 40 mm from the nozzle tip. This can be explained by the coalescence of large fast droplets, with slower smaller ones. The decrease of V for $z > 40$ mm results from droplet deceleration due to drag as droplets move through quiescent air[8,9].

The variation of spray temperature with distance for all nozzles shown in Fig. 2c is to be anticipated. Sprays produced by smaller I.D. nozzles are more finely atomized, i.e., have a larger surface area, removal of latent heat of vaporization from the remaining liquid droplets is more effective and, thus, somewhat lower spray temperatures are achieved. Notice that the initial temperature T_0, does not seem to be the same for all nozzles. For example, for the W nozzle (nozzle with the largest I.D.), T_0 is close to -26°C, which coincides with the boiling temperature of the cryogen, and is the expected cryogen temperature after a sudden expansion through the valve (provided evaporation within the hose and nozzle are negligible). This means that the cryogen has not been significantly atomized and, thus, that the liquid cryogen has not been able to undercool. On the other hand, the T_0 estimated for the GL nozzle (nozzle with the smallest I.D.) is equal to -49°C, which indicates better atomization right at the exit of the nozzle (and perhaps even some degree of evaporation within the nozzle) and, therefore, a larger undercooling.

An interesting observation is that the ratio between the N and the GL nozzle diameters is 1.4, and no significant differences are appreciable in terms of their droplet diameter and temperature evolutions. On the other hand, the ratio between the N and the W nozzle I.D. is slightly greater (2.0), and yet the differences in terms of their droplet diameter and temperature evolutions are noteworthy. This large change in spray characteristics for a relatively similar nozzle diameter ratio indicates that there is a critical nozzle diameter—somewhere between 0.8 and 1.4 mm, at which a change in the atomization mechanism takes place (at least, for the particular conditions under which this cryogen is sprayed).

This study shows that variations of h can be achieved by positioning the nozzles at different distances from the skin surface, and even more significant variations can be achieved by varying the nozzle diameter. The effect of nozzle-to skin distance (z) in the resulting h is shown in Fig. 2d. Our results demonstrate that values between 6,000 to 8,400 W/m^2 K may be obtained for the SP and GL nozzles in the range of z between 30 and 50 mm. Significantly larger values of h may be obtained by increasing nozzle diameter to about 1.4 mm (W nozzle). In a previous study[7], the differences in h due to changes in nozzle diameter were attributed to build up of a cryogen layer on the sprayed surface, which appeared to be thicker in the case of the N nozzle as compared with the W nozzle, and thus constituted a higher thermal barrier for heat extraction. It was speculated then that the different cryogen layer thicknesses were due to the larger momentum (given by the product of D and V) of large and fast moving droplets, such as those produced by W nozzle, in contrast to the smaller and slower moving droplets produced by N nozzle. This hypothesis is supported in this study by the larger droplet diameter and velocity seen for the W nozzle in comparison with the SP, GL, and N nozzles (Figs. 2a and 2b). Additionally, note that T starts to increase between 80 and 120 mm for the SP, GL, and N nozzles. This increase is consistent with D and V measurements, since the higher momentum droplets move further downstream before evaporating completely. Clearly, the complexity of the problem is such that establishing a correlation between D, V, T, and h, is not straightforward. Nevertheless, it is noted that a relatively invariant value of h is reached between 40 and 70 mm for the SP and GL nozzles, the same range where D is maximum. This is perhaps an indication that the influence of D on h may actually be more dominant than that of V.

For laser therapy of PWS or other superficial targets, it is important that the effect of cooling remains spatially confined to the superficial 100–200 μm of the skin[2,19]. Such spatial selectivity requires the use of short cryogen spurts and the highest possible heat transfer rates. Therefore, aiming at the highest h a nozzle can produce, should be the most important criterion to determine its appropriate position with respect to the skin surface. One should be aware, however, that the use of larger

diameter nozzles may not be viable for clinical applications, since they produce more confined jet-like sprays, and larger droplet momentum may produce patient discomfort. In contrast, smaller diameter nozzles produce a finely atomized spray, which is more acceptable to patients and cover a wider sprayed area. The downside of fine atomization is, as mentioned above, that it may induce the formation of a thicker liquid layer, which adversely affects the heat extraction rate due to low thermal conductivity of cryogen[20]. Maximizing h may not be the ultimate goal for CSC aimed at therapy of deeper targets (e.g., hair removal). In fact, the GL nozzle is currently used with an Alexandrite laser for the treatment of deep targets and for such targets, it may actually be beneficial to reduce h in order to have a more prolonged and less aggressive heat extraction, while still obtaining sufficient epidermal protection[5,21].

The results presented in Fig. 3 demonstrate that for very light skin (μ_a=8 cm^{-1}), even a heat transfer coefficient of 2,400 W/m^{2}K^3, would provide sufficient epidermal protection, while significant PWS damage would be obtained. In fact, an increase in h to values similar to those measured for the SP and GL nozzles (≈ 6,000 W/m^{2}K), would further reduce the epidermal damage, while sufficient PWS thermal damage would still be induced. For slightly darker skin types, e.g., μ_a = 20 cm^{-1}, the increase in epidermal temperature could be significant for the dose used (13 J/cm^2), as exemplified in Figs. 4 and 5. Fig. 4 shows that a post-cooling with an h value similar to the maximum measured for the SP nozzle, would help reduce the epidermal damage by a small amount only (≈ 2%), while the PWS damage would be basically unaffected but yet large enough to induce irreversible thermal damage. In Fig. 5 the heat transfer coefficient was increased from 8,400 W/m^{2}K to the upper estimate value we have previously reported (30,000 W/m^{2}K)[7] and post-cooling was applied in both cases. As seen in Table 5, for this choice of parameters the epidermal damage is significantly minimized (by more than a factor of 170) and, although the PWS damage is also reduced, it is still be large enough to induce the desired thermal damage. This is a good example of the importance of maximizing h to be able to treat skin types that may be otherwise not viable. Finally, Fig. 6 shows that for darker skin types (μ_a = 52 cm^{-1}), the increase in epidermal temperature with a dose of 10 J/cm^2 would be excessive, and yet no significant damage would be induced to the PWS. Even an increase in h up to 60,000 W/m^2 K and post-cooling, would not be sufficient to avoid extensive epidermal damage.

5. CONCLUSIONS

This study shows that variations of the heat transfer coefficient, h, can be achieved by positioning nozzles at different distances from the skin surface, and significant increases in h can also be achieved by increasing nozzle inner diameter (I.D.) For the SP and GL nozzles, variations in the heat transfer coefficient are larger than those in the spray temperature and, therefore, maximization of the heat flux—which is needed to improve PWS treatments for skin types III and higher, should be determined by adjusting the nozzle-to-skin distance within the range where the heat transfer coefficient is maximized rather than that at which the spray temperature is minimized. Sprays produced by all the studied nozzles appear to reach very similar minimal temperatures (≈ -60^{o}C), but for nozzles with I.D. ranging from 0.5 to 0.8, relatively invariant values of h are reached within the ranges of z where D is maximal. This suggests that the influence of droplets mass (D) may actually be the most determinant variable on the value of h.

Preliminary results of a heat diffusion numerical simulation using a Monte Carlo technique to determine laser energy absorption and distribution within human skin, indicate that for light skin types (μ_a = 8 cm^{-1}), h values that are measured for commercial devices (5,000 to 10,000 W/m^{2}K) are large enough to offer adequate epidermal protection, while enduring PWS photothermal damage. For somewhat darker skin types (e.g., μ_a= 20 cm^{-1}), an increase in h would significantly help reduce the risk for epidermal damage for doses beyond 12 J/cm^2, while the benefits of using post-cooling would be minimal. Unfortunately, however, not even an increase in h to about 60,000 W/m^{2}K and post-cooling would be sufficient to avoid severe epidermal damage for skin types where μ_a = 52 cm^{-1} or higher.

ACKNOWLEDGEMENTS

This work was supported by a research grant from the Institute of Arthritis and Musculoskeletal and Skin Diseases at the National Institutes of Health (AR43419 to JSN), and in part by the Slovenian Ministry of Science and Technology (BM). Institutional support from the Office of Naval Research, Department of Energy, National Institutes of Health, and the Beckman Laser Institute and Medical Clinic Endowment is also acknowledged. We also acknowledge the grant from National Science Foundation for the purchase of the PDPA system (CTS-9901375 to EJL).

REFERENCES

1. W. Verkruysse, B. Majaron, B.S. Tanenbaum, and J.S. Nelson, "Optimal cryogen spray cooling parameters for pulsed laser treatment of port wine stains," Lasers Surg. Med. 27, pp. 165-170, 2000.
2. J.S. Nelson, T.E. Milner, B. Anvari, B.S. Tanenbaum, S. Kimel, L.O. Svaasand, and S.L. Jacques, "Dynamic epidermal cooling during pulsed laser treatment of port-wine stain. A new methodology with preliminary clinical evaluation," Arch. Dermatol. 131, pp. 695-700, 1995.
3. J.H. Torres, J.S. Nelson, B.S. Tanenbaum, T.E. Milner, D.M. Goodman, and B. Anvari, "Estimation of internal skin temperature measurements in response to cryogen spray cooling: implications for laser therapy of port wine stains", IEEE J Special Topics Quant Elect, 5, pp.1058-1066, 1999.
4. G.B. Altshuler, H.H. Zenzie, A.V. Erofeev, M.Z. Smirnov, R.R. Anderson, and C. Dierickx, "Contact cooling of the skin", Phys Med Biol, 44, pp.1003-1023, 1999.
5. B. Majaron, S. Kimel, W. Verkruysse, G. Aguilar, K. Pope, L.O. Svaasand, E.J. Lavernia, and J.S. Nelson, "Cryogen spray cooling in laser dermatology: effects of ambient humidity and frost formation," Lasers Surg. Med. 28 (2), 2001 – in press.
6. J.W. Tunnell, J.S. Nelson, J.H. Torres, and B. Anvari, "Epidermal protection with cryogen spray cooling during high fluence pulsed dye laser irradiation: an ex vivo study", Lasers Surg. Med. 27, pp. 373-383, 2000.
7. W. Verkruysse, B. Majaron, G. Aguilar, L.O. Svaasand, and J.S. Nelson, "Dynamics of cryogen deposition relative to heat extraction rate during cryogen spray cooling," in: Lasers in Surgery: Advanced Characterization, Therapeutics, and Systems X, Proc. SPIE 3907, pp. 37-48, Bellingham, WA, 2000.
8. G. Aguilar, W. Verkruysse, B. Majaron, Y. Zhou, J.S. Nelson, and E.J. Lavernia, "Modeling cryogenic spray temperature and evaporation rate based on single-droplet analysis", Proceedings of the Eighth International Conference on Liquid Atomization and Spray Systems, Pasadena CA, July 16-20, CD-ROM, pp.1041-1046, 2000.
9. G. Aguilar, B. Majaron, W. Verkruysse, Y. Zhou, J.S. Nelson, and E.J. Lavernia, "Theoretical and experimental analysis of droplet diameter, temperature, and evaporation rate evolution in cryogenic sprays", Int. J. of Heat and Mass Transfer,2001—in press.
10. D. Paithankar, J. Hsia, and E.V. Ross, "Sub-surface wrinkle removal by laser treatment in combination with dynamic cooling" in: Lasers in Surgery: Advanced Characterization, Therapeutics, and Systems X, Proc. SPIE 3907, pp. 4-11, Bellingham, WA, 2000.
11. T.J. Pfefer, D.J. Smithies, T.E. Milner, M.J.C. van Gemert, J.S. Nelson, and A.J. Welch, "Bioheat transfer analysis of cryogen spray cooling during laser treatment of port wine stains", Lasers Surg. Med. 26, pp. 145-157, 2000.
12. L. Wang and S.L. Jacques, "Monte Carlo Modeling of Light Transport in Multi-layered Tissues in Standard C", 1992, University of Texas M. D. Anderson Cancer Center.
13. G. Aguilar, B. Majaron, W. Verkruysse, J.S. Nelson, and E.J. Lavernia, "Characterization of cryogenic spray nozzles with application to skin cooling," J. Heat Transfer (submitted).
14. A.H. Lefevbre, "Atomization and Sprays" (1st Edn). New York: Taylor & Francis. 1989: 309.
15. S.L. Jacques, R.D. Glickman, and J.A. Schwartz, "Internal absorption coefficient and threshold for pulsed laser disruption of melanosomes isolated from retinal pigment epithelium", Proc. SPIE 1996: vol 2681, pp. 468-477.
16. G. Aguilar, B. Majaron, W. Verkruysse, J.S. Nelson, and E.J. Lavernia, "Characterization of cryogenic spray nozzles with application to skin cooling," Proc. ASME, FED-253, pp. 189-197, New York, 2000. (Internat. Mechanical Engineering Congress, Orlando, FL, Nov. 2000.
17. M.Orme, "Experiments on droplet collisions, bounce, coalescence and disruption", Progress in Energy and Combustion Science, 23, pp.65-79, 1997.
18. R. Nishitani, A. Kasuya, and Y. Nishina, "Insitu STM observation of coalescence of metal particles in liquid", Zeitschrift fur Physik D, 26, pp.S42-S44,1993.
19. J.S. Nelson, T.E. Milner, B. Anvari, B.S. Tanenbaum, L.O. Svaasand, and S. Kimel, "Dynamic epidermal cooling in conjunction with laser-induced photothermolysis of port wine stain blood vessels", Lasers Surg Med, 19, pp.224-229, 1996.
20. K.A. Estes, I. Mudawar, "Correlation of Sauter mean diameter and critical heat flux for spray cooling of small surfaces," Int. J. Heat Mass Transfer 38, pp. 2985-2996, 1995.
21. J.S. Nelson, B. Majaron, and K.M. Kelly, "Active skin cooling in conjunction with laser dermatologic surgery: Methodology and clinical results", Seminars Cutaneous Med Surg, 19, N4, pp. 253-266, 2000.